

1 A new late Aptian elasmosaurid from the Paja Formation, Villa de Leiva, Colombia

2
3 Maria Eurídice Páramo-Fonseca¹; José Patricio O'Gorman^{2,3} Zulma Gasparini^{2,3} Santiago
4 Padilla⁴ and Mary Luz Parra Ruge⁴

5
6 ¹Departamento de Geociencias, Universidad Nacional de Colombia, Carrera 30 No 45-03, Bogotá, Colombia.

7 meparamof@unal.edu.co

8 ²División Paleontología Vertebrados, Museo de La Plata, Universidad Nacional de La Plata, Paseo del Bosque
9 s/n., B1900FWA, La Plata, Argentina.

10 ³ CONICET: Consejo Nacional de Investigaciones Científicas y Técnicas, Argentina.

11 joseogorman@fcnym.unlp.edu.ar; zgaspari@fcnym.unlp.edu.ar.

12 ⁴Centro de Investigaciones Paleontológicas, Villa de Leiva, Boyacá, Colombia. info@centropaleo.com;

13 mlparra@centropaleo.com .

14
15 **Corresponding author:** María Eurídice Páramo-Fonseca

16
17 Declaration of interest: none

18
19 **Abstract:** A new genus and species of elasmosaurid, *Leivanectes bernardo* gen. et sp.

20 nov., from the upper Aptian levels of the Paja Formation of Villa de Leiva (Boyacá,

21 Colombia) is described. The new elasmosaurid is characterized by a short mandibular

22 symphysis, bears only three alveoli (there are five in *Callawayasaurus colombiensis*), has

23 an enlarged premaxillary alveoli, and has a mandible that includes only seven alveoli in

24 each ramus anterior to the orbit (there are 11 in *Callawayasaurus colombiensis*). This new

25 elasmosaurid taxon has fewer and larger alveoli than any other presently described

26 elasmosaurid taxon. The observed differences indicate that the new species consumed
27 larger-bodied prey than did other elasmosaurids. The new taxon suggests that the
28 elasmosaurids were diverse in the Colombian late Aptian sea.

29 **Key words:** Plesiosauria, Elasmosauridae, Lower Cretaceous, Aptian, Villa de Leiva,
30 Colombia.

31

32 1. INTRODUCTION

33 Colombia is one of the richest South American countries in Lower Cretaceous marine
34 reptiles. This richness is not only evident in their taxonomic diversity but also in the
35 quantity and quality of the specimens (Páramo-Fonseca, 2015). The records are mainly
36 concentrated in the Lower Cretaceous beds of the Villa de Leiva area (Boyacá-central
37 Colombia), where three-dimensionally preserved and often articulated remains of
38 plesiosaurians, ichthyosaurians and sea turtles are present (Gómez-Pérez and Nòe, 2017;
39 Maxwell et al., 2015; Páramo-Fonseca, 2015; Páramo-Fonseca et al., 2016). The
40 stratigraphic horizons in which these specimens are found are the Barremian and upper
41 Aptian units of the Paja Formation, which are informally referred to as “nivel de arcillolitas
42 abigarradas” (Etayo-Serna, 1968; Forero and Sarmiento, 1985). In addition to the
43 exceptional preservation of most specimens, the successful preparation of many specimens
44 by means of chemical and manual techniques (Padilla et al., 2010) allow for more detailed
45 anatomical studies.

46 The plesiosaurs from Villa de Leiva are represented mainly by pliosaurids; however, some
47 remains of elasmosaurids have also been found (Páramo-Fonseca, 2015). Welles (1962)

48 described and named the first elasmosaurid from northern South America, which was found
49 in Villa de Leiva, was “*Alzadasaurus*” *colombiensis*, which subsequently was established
50 as a distinct genus, *Callawayasaurus colombiensis*, by Carpenter (1999). Fragments of a
51 skull and a mandible of a second elasmosaurid were also referred to as “*Alzadasaurus*”
52 *colombiensis* (Goñi and Gasparini, 1983; these remains are currently under review by MEP-
53 F). A new elasmosaurid specimen (FCG-CBP-22) from Villa de Leiva was recently
54 prepared and is the subject of this study. It was donated by Mr. José Sierra to the Fundación
55 Colombiana de Geobiología in 1999 and is housed in the collections of the Centro de
56 Investigaciones Paleontológicas in Villa de Leiva.

57 Specimen FCG-CBP-22 comprises the anterior section of a skull, with the jaws preserved
58 in occlusion. It was collected from Loma La Cabrera, approximately 4 km west of Villa de
59 Leiva. The exact location of the discovery site is not known; however, specimen FCG-
60 CBP-22 was recovered from beds of the “nivel de arcillolitas abigarradas” of the Paja
61 Formation. A small ammonite conch (FCG-CBP-46) was found in the surrounding matrix
62 (Fig. 1C). The phase of tubercles development in this ammonite is comparable to that
63 which was observed in smaller individuals (up to 35 mm diameter) of *Chelonicerias*
64 (*Epicheloniceras*) *carlosacostai* Etayo-Serna, 1979 (cf. Etayo-Serna, 1979, pag. 34), which
65 characterize the upper Aptian in Colombia (Etayo-Serna, pers. comm.).

66

67 2. METHODS

68 Specimen FCG-CBP-22 was prepared by one of the authors (MLPR), using mechanical and
69 chemical techniques. To maintain the integrity of the fossil, a special treatment was

70 implemented to eliminate acidic and saline residues after acid preparation. The chemical
71 procedure included immersions in 2% sulfamic acid followed by washes under running
72 water for two days and submersion of the fossil into deionized water in a hermetic
73 container. This process was repeated until a stable pH measurement was obtained. A
74 detailed description of the method is found in Padilla et al. (2010).

75 The new specimen FCG-CBP-22 is an incomplete skull with the mandible preserved in
76 occlusion. Because of its distinctively large alveoli, a comparison with other elasmosaurids
77 focused on mesodistal measurements of alveolar size. The nomenclature used for alveoli
78 measurements follows that of Smith and Dodson (2003: fig. 7).

79 FCG-CBP-22 was added to the Plesiosauria data set of O’Gorman and Coria (2016), which
80 is based on that of O’Gorman (2016a), which in turn is based on Benson and Druckenmiller
81 (2014). The character states of the new specimen are shown in Appendix I. Four OTUs
82 were also incorporated to the data set: *Eromangasaurus australis* (Sachs, 2005),
83 *Zarafasaurus oceanis* Vincent, Bardet, Pereda Suberbiola, Bouya, 2011, and *Nakonanectes*
84 *bradti* Serratos, Druckenmiller and Benson, 2017, following the scoring of Serratos et al.
85 (2017: supplemental data), and *Lagenanectes richterae* Sachs, Hornung and Kear, 2017,
86 following the scoring of Sachs et al. (2017: supplemental data). The scoring of *Styxosaurus*
87 *snowii* (Williston, 1890) was modified according to Sachs et al. (2018: appendix). Mesquite
88 Software (Maddison and Maddison, 2011) was used to compile the new data, which
89 comprises 95 OTUs and 276 characters, from which the phylogenetic analysis was carried
90 out. All characters were considered to be unordered. The cladistic analysis was run on TNT
91 (v1.5) (Goloboff and Catalano, 2016). A heuristic search with the TBR algorithm (tree
92 bisection reconnection) recovering 20,000 trees was performed. An initial exploration for a

93 search of the shortest trees islands used Wegner trees (1000 random-addition sequence
94 replicates, 1000 saved trees per replication and three random seeds). The resulting subset of
95 most parsimonious trees (MPTs) was used as the initial group of trees for a TBR search. A
96 strict consensus was applied, and the IterPCR algorithm was run to determine and prune the
97 unstable OTUs in the consensus (Pol and Escapa, 2009). The consistency (CI) and retention
98 (RI) indexes (Farris, 1989) were calculated, and Bremer support values (Bremer 1994) were
99 computed for some nodes in the reduced consensus cladogram.

100 **2.1 Institutional Abbreviations**

101 **BGR**, Bundesanstalt für Geowissenschaften und Rohstoffe, Hannover, Germany; **FCG-**
102 **CBP**, Fundación Colombiana de Geobiología, Centro de Investigaciones Paleontológicas;
103 **ICNMHN**, Instituto de Ciencias Naturales, Universidad de Colombia, Bogotá, Colombia;
104 **KUVP**, Kansas University, Vertebrate Paleontology, United States; **NPC**, National
105 Paleontological Collection, Lower Hutt, New Zealand; **NSM**, National Science Museum,
106 Tokyo, Japan; **OCP**, Office Chérifien des Phosphates, Khouribga, Morocco; **QM**,
107 Queensland Museum, Brisbane, Australia; **RSM**, Royal Saskatchewan Museum, Regina,
108 Saskatchewan, Canada; **SMUSMP** Southern Methodist University, Shuler Museum of
109 Paleontology, Dallas, USA; **UCPM**, University of California Museum of Paleontology,
110 California, USA; **UNSM**, University of Nebraska State Museum, Lincoln, USA.

111 **2.2 Unique digital ZooBank registration identifier:**

112

113 **3. SYSTEMATIC PALEONTOLOGY**

114 SAUROPTERYGIA Owen, 1860

115 PLESIOSAURIA de Blainville, 1835

116 PLESIOSAUROIDEA Welles, 1943

117 ELASMOSAURIDAE Cope, 1869

118 *Leivanectes* gen. nov.

119 *LSID*:

120 Type and only species: *Leivanectes bernardo* sp. nov.

121 **Diagnosis:** For type and only known species.

122 **Derivation of name:** From Villa de Leiva, which is the locality where the holotype was
123 collected, and Greek *nektos*, swimmer.

124 *Leivanectes bernardo* sp. nov.

125 *LSID*:

126 **Holotype:** FCG-CBP-22. Anterior half of the skull comprising the rostrum, part of the
127 orbital area and anterior half of the mandible.

128 **Type locality and horizon:** Loma La Cabrera, Villa de Leiva, Department of Boyacá,
129 central Colombia. Upper section of the “nivel de arcillolitas abigarradas” of the Paja
130 Formation (Etayo-Serna, 1968), upper Aptian (Etayo-Serna, pers. comm.) (Fig. 1).

131 **Derivation of name:** In honor of Dr. Carlos Bernardo Padilla, who is recently deceased and
132 who dedicated part of his life to the rescue and preservation of fossils mainly from the area
133 of Villa de Leiva. Dr. Carlos Bernardo Padilla is the founder, along with his brother

134 Santiago Padilla, of the prestigious Centro de Investigaciones Paleontológicas in the town
135 of Villa of Leiva, Colombia.

136 **Differential diagnosis:** Elasmosaurid with the following combination of features:
137 premaxilla without dorsal medial ridge, differing from *Callawayasaurus colombiensis*,
138 *Eromangasaurus australis*, and Late Cretaceous elasmosaurids; meso-distal measurement
139 of the third and fourth premaxillary alveoli approximately 14% of the preorbital length,
140 differing from the smaller alveoli that was recorded for *Callawayasaurus colombiensis*,
141 *Tuarangisaurus keyesi* and aristonectines; three alveoli pairs adjacent to the mandibular
142 symphysis, a feature shared with *Terminonatator ponteixensis*; five premaxillary alveoli,
143 which differs from that of *Elasmosaurus platyurus* (6+) and *Eromangasaurus australis* (3-
144 4); vomers lacking a posterior medial V-shaped notch near the internal nares to
145 accommodate the pterygoids, which differs from that of *Lagenanectes richterae* and
146 *Morturneria seymourensis*; seven mandibular alveoli anterior to the orbit, which differs
147 from *Callawayasaurus colombiensis* (~11), *Futabasaurus suzukii* (~12), *Libonectes*
148 *morgani* (~10), *Styxosaurus* spp (9+), *Terminonatator ponteixensis* (~10), *Thalassomedon*
149 *haningtoni* (~10), and *Tuarangisaurus keyesi* (~10); absence of a dentary ventral
150 elaboration along the mandibular symphysis, which differs from that of *Callawayasaurus*
151 *colombiensis*, *Eromangasaurus australis*, *Lagenanectes richterae* and *Zarafasaurus*
152 *oceanis*; and elliptical external nares, which differs from the cordate external nares of
153 *Nakonanectes bradti*.

154

155 4. DESCRIPTION

156 **4.1 Cranium**

157 FCG-CBP-22 is an incomplete skull with its mandible preserved in occlusion. The most
158 anterior part of the specimen including the rostrum and mandibular symphysis is well
159 preserved and undeformed. The interorbital part of the skull roof is dorsoventrally crushed
160 (Fig. 2).

161 **Premaxilla:** Both premaxillae are well preserved and form almost the entire rostrum. The
162 rostrum is wide and dorsally convex in the cross section. The premaxilla lacks a medial
163 ridge, as it does in *Futabasaurus suzukii* Sato, Hasegawa and Manabe, 2006, *L. richterae*
164 and basal plesiosauroids (Benson and Druckenmiller, 2014; Sachs et al., 2017; Sato et al.,
165 2006; Serratos et al., 2017). The midline suture is visible along the entire premaxillary
166 length, with the exception of its anteriormost tip. The premaxilla forms the anterior and
167 medial margin of the external naris (Fig. 2). Each premaxilla bears five alveoli that create a
168 slightly waved margin in a lateral view. A change in the alveoli size is observed at the
169 premaxilla-maxilla contact, but there is no diastema (Fig. 2B). The dorsomedial process of
170 the premaxilla is progressively higher toward the internarial sector (Fig. 2C). The
171 dorsomedial process is broken at the level of the anterior border of the orbit and appears to
172 be projected over the frontals; however, its posterior extension remains unknown. The
173 dorsal surface of the premaxilla is slightly wrinkled and bears a neurovascular foramina
174 that are randomly distributed, three of which are larger and aligned near the midline.

175 **Maxilla:** The premaxilla-maxilla suture is slightly curved along its length. The maxillae
176 form the ventral margin of the external nares and the anterolateral margin of the orbit (Fig.
177 2C). In the lateral view, the alveolar border of the maxilla shows a slight ventrally convex

178 curve that includes the 1st to the 4th alveoli. Although incomplete, the left maxilla bears nine
179 alveoli. In the palatal view, the anterior part of the maxillae is not well exposed, but its
180 contact with the vomers is insinuated. The maxilla-palatine junction is barely visible on
181 both sides of the skull, and it begins at the posterior rim of the internal naris. The maxilla
182 forms the lateral margin of the internal naris (Fig. 2D).

183 **External naris:** Both external nares are poorly preserved along the posterior border (Fig.
184 2C). The external naris is located at the level of the second maxillary alveolus. The distance
185 from the external naris to the midline of the skull is equivalent to the width of the external
186 naris, which is shorter than that of *F. suzukii* and *N. bradti* (Sato et al., 2006; Serratos et al.,
187 2017). The distance from the external naris to the orbit is as short as it is in
188 *Callawayasaurus colombiensis* (Welles, 1962) and in *E. australis* (Kear, 2005: fig. 6;
189 Sachs, 2005a: fig. 3A; Welles, 1962: fig. 3) and is shorter than that in *F. suzukii* (Sato et al.,
190 2006). The participation of the frontal in the narial margins cannot be established due to the
191 poor preservation of this area.

192 **Orbit:** Both orbits are incomplete. Their posterior region is missing. The preserved orbital
193 areas are slightly expanded laterally (Fig. 2C). The presence of a dorsally convex ventral
194 margin of the orbit, a feature that is common among elasmosaurids (Benson and
195 Druckenmiller, 2014; Carpenter, 1999), cannot be established due to the poor preservation
196 of this margin.

197 **Frontal:** Both frontals are partially crushed and, therefore, an accurate description of these
198 bones cannot be given. The frontal forms an expanded table over the orbits, as in *C.*
199 *colombiensis* (Welles, 1962), but its relationship with the dorsomedial process of the

200 premaxilla remains unclear. The right frontal contacts posteriorly a small preserved portion
201 of the parietal (Fig. 2C).

202 **Prefrontal:** A fragment of each prefrontal is exposed on both sides of the skull. Both
203 prefrontals are broken and are slightly displaced from their anatomical place. The prefrontal
204 forms part of the anterior margin of the orbit (Fig. 2C), as in *N. bradti* (Serratos et al.,
205 2017). Their poor preservation prevents the establishment of the shape and extension of this
206 element.

207 **Postfrontal:** The postfrontals are only represented by two small bone fragments that are
208 badly preserved on the posterior region of the orbits (Figs. 2B, C).

209 **4.2 Palate**

210 The palate is incomplete and is partially covered by the mandibular rami. It preserves the
211 anterior process of the pterygoids, the anterior part of the palatines and the posterior portion
212 of the vomers.

213 **Vomer:** The anterior end of the vomers is not visible, because the mandible is in occlusion.
214 Both vomers are united, but they are not completely fused along the midline. In its middle
215 region, the vomer is narrow and forms the medial margin of the internal naris. The vomer
216 extends posterior to the internal naris, as is common in elasmosaurids (Carpenter, 1997: fig.
217 2D; O'Gorman et al., 2017: fig. 7B; O'Keefe, et al., 2017: fig. 4C; Sato et al., 2006: fig. 4C;
218 Vincent et al., 2011: fig. 2D, E; Welles, 1962: fig. 4A). The posterior region of the vomer is
219 limited laterally, with the palatine through an irregular suture, and medially with the
220 anterior margin of the pterygoid. The vomers are not separated by the pterygoids along the

221 midline (Fig. 2D), which is a condition that is also seen in *F. Suzukii*, *Libonectes morgani*
222 (Welles, 1949) and *Z. oceanis* (Sato et al., 2006; Vincent et al., 2011; Welles, 1949: Plate
223 3).

224 **Palatine:** Both palatines are incomplete. The preserved portion of each palatine is a flat to
225 slightly convex plate that medially contacts the pterygoid and the vomer (Fig. 2D).

226 Although the suture with the maxilla is not clear on either side, the anterior end of the
227 palatine narrows and appears to form the posterior border of the internal naris, which is
228 known in other elasmosaurids (Carpenter, 1997: fig. 2D; O'Gorman et al., 2017: fig. 7B;
229 Sachs et al., 2017: fig. 3; Sato et al., 2006: fig. 4C; Vincent et al., 2011: fig. 2D, E; Welles,
230 1962: fig. 4A).

231 **Pterygoid:** Only the anterior process of the pterygoid is preserved. The pterygoid medially
232 joins its counterpart, anteriorly joins the vomer and laterally joins the palatine. In the
233 ventral view, the pterygoids form a concave area between the palatines. However, this
234 appears to be a taphonomic feature (Fig. 2D).

235 **Internal naris:** The internal naris is not entirely distinguishable. It is approximately 20 mm
236 in length and 8 mm in width. Each internal naris is limited by the maxilla, the vomer and
237 probably the palatine to a limited extent (Fig. 2D).

238 4.3 Mandible

239 **Dentary:** The dentaries are fused along the mid-line of the symphysis (Fig. 2C) and,
240 because the mandible is in occlusion, it is difficult to see if this fusion is also complete on
241 the dorsal surface of the symphysis. In the ventral view, the external surface of dentaries is

242 marked by a great quantity of pits at the symphyseal region, which differs from the less
243 densely distributed pits that cover the external surface of each mandibular ramus (Figs. 2A,
244 B, D). The ventral surface of the dentaries along the mandibular symphysis lacks any
245 elaboration (Figs. 4C, E), such as in *L. morgani* and *N. bradti* (Serratos et al., 2017;
246 Welles, 1949), and differs from *E. australis*, *L. morgani* and *S. snowii*, in which a
247 symphyseal keel is observed (Kear, 2007; Sachs and Kear, 2017; Sachs et al., 2018: fig.
248 3B). In the lateral view, the symphysis includes only three pairs of large alveoli for
249 functional teeth, as in *Terminonatator ponteixensis* Sato 2003, *S. snowii* and *N. bradti*
250 (Sachs et al., 2018; Sato, 2003; Serratos et al., 2017). In the anterior view, there are two
251 pairs of alveoli that are anteriorly directed, which is similar to the premaxillae (Fig. 2A).

252 **Angular:** The anterior end of both angulars is preserved. In the ventral view, the angular is
253 exhibited posterior to the level of the internal nares (Fig. 2D) but less posterior than in *T.*
254 *ponteixensis* or *N. bradti* (Sato, 2003; Serratos et al., 2017). In the medial view, the anterior
255 end of the angular forms a wedge that anteriorly tapers against the splenial, posterior to the
256 mandibular symphysis.

257 **Splenial:** The preserved portion of the splenials forms a long and narrow blade tapering
258 anteriorly. The splenials end where the symphysis begins, as in *L. morgani* (Welles, 1949).

259 **Coronoid:** The coronoid forms the dorsal half of the medial wall of the preserved part of
260 the mandible and extends anteriorly to approximately 2 cm posterior to the symphysis, as in
261 *L. morgani* (Welles, 1949). The anterior end of the coronoid contacts the dentary in an S-
262 shaped suture.

263 **4.4 Alveoli and dentition**

264 The alveoli of the upper jaw differ in size. Their mesodistal measurements are shown in
265 Table 1. The first premaxillary alveolus is procumbent and small but is not significantly
266 smaller than the second. However, its diameter is less than half that of the third alveolus
267 (Table 1). This condition is found in *L. richterae* (Sachs et al., 2017), *S. snowii* (Sachs et
268 al., 2018: Appendix) and *T. ponteixensis* (Sato, 2003). The third alveolus is the largest and
269 is similar to the fourth, while the fifth is smaller. The more complete left maxilla bears nine
270 alveoli and, extrapolating the possible length of the missing part, and it is probable the total
271 number of alveoli was approximately eleven. The alveoli of this maxilla are of different
272 sizes, which indicates a heterodont dentition. The first is relatively small compared with the
273 others that are variable in size (see Table 1). There are twelve alveoli in the left mandibular
274 ramus and eleven on the right. The seven anterior alveoli are similar in size and those that
275 are more posterior are smaller.

276 Twelve fragmentary teeth are preserved, seven of which are almost complete and five that
277 are broken at their crown base. The surfaces of the teeth are damaged, and only their labial
278 surfaces can be observed. The crown is conical in shape and circular in the cross section, as
279 in *C. colombiensis* and *L. richterae* (Sachs et al., 2017; Welles, 1962). The surface of the
280 enamel is practically smooth. However, on the labial side of the more complete tooth, very
281 slight ridges and transversal wrinkles in the basal two-thirds of the crown are present (Fig.
282 2E), which is similar to those described by Welles (1949) for the teeth of *L. morgani*.

283

284 5. DISCUSSION

285 5.1 Morphological comparisons

286 The specimen FCG-CBP-22 shows well-ossified elements and some closed sutures, such as
287 the symphysis, which indicates that the individual was osteologically mature at the time of
288 death (sensu Brown, 1981).

289 Although the specimen FCG-CBP-22 is an incomplete skull and does not preserve any of
290 the autapomorphic characteristics of Elasmosauridae, some of the cranial features
291 registered as diagnostic of elasmosaurids (Brown, 1981; Ketchum and Benson, 2010;
292 O’Keeffe, 2001; Vincent et al., 2011) are present including vomer extended posterior to the
293 internal nares (O’Keeffe, 2001), splenial without participation in the mandibular symphysis
294 (Ketchum and Benson, 2010) and absent of an anterior interpterygoid vacuity (Vincent et
295 al., 2011). The new specimen also presents the following two features that together indicate
296 its elasmosaurid affinities: a nonelongated rostrum and premaxilla dorsomedial process
297 projecting over the frontals. These characteristics are present in all elasmosaurids, with the
298 exception of *Callawayasaurus colombiensis*, in which the premaxilla tapers more
299 proximally (Benson and Druckenmiller, 2014; J.P.O’G Pers. Obs.).

300 The early Cretaceous elasmosaurids that can be compared with *L. bernardoii* include the
301 late Aptian *C. colombiensis* UCMP 38349 (Figs. 3C-E and 4A-D), and UCMP 125328
302 (Figs. 4E-F) from Villa de Leiva (Welles, 1962), the Albian *E. australis* from Australia
303 (Kear, 2005, 2007; Sachs, 2005a), and the late Hauterivian *L. richterae* from Germany
304 (Sachs et al., 2017). The more distinctive feature of the new taxon *L. bernardoii* is the
305 presence of large alveoli that result in a lower number of alveoli in the different regions of
306 the cranium and mandible. *L. bernardoii* has five premaxillary alveoli, which differs from
307 the maximum of four premaxillary alveoli in *E. australis*, (Kear, 2007) and the minimum of
308 six premaxillary alveoli in *Elasmosaurus platyurus* Cope, 1868 (Sachs, 2005b). In Table 2

309 the alveolar account of *L. bernardoi* (FCG-CBP-22) is contrasted with that of the Early
310 Cretaceous elasmosaurids and other comparable Late Cretaceous elasmosaurids, which
311 have 4-5 premaxillary alveoli (*F. suzuki*, *L. morgani*, *Thalassomedon haningtoni* Welles,
312 1943, *Tuarangisaurus keyesi* Wiffen and Moisley, 1986, *Z. oceanis*, *T. ponteixensis*,
313 *Styxosaurus browni* Welles, 1952, *S. snowii* and *N. bradti*). *L. bernardoi* have the same
314 number of alveoli pairs on the mandibular symphysis (three alveoli) as *T. ponteixensis*, *S.*
315 *snowii* and *N. bradti*. It has seven mandibular alveoli anterior to the orbit, while all the
316 other taxa have more than seven.

317 *L. bernardoi* is different from other elasmosaurids, except for *N. bradti*, in the ratio
318 between the mesiodistal measurements of the premaxillary alveoli and the preorbital length
319 (Figs. 3A, B). In *L. bernardoi*, the meso-distal measurement of the third and fourth
320 premaxillary alveoli is approximately 14% of the preorbital length. Although no
321 measurements were taken, this ratio seems to be similar in *N. bradti* (Serratos et al., 2017:
322 fig. 2) and different in other elasmosaurids, such as the Lower Cretaceous *C. colombiensis*
323 (~6%), *E. australis* (~8%) (Kear, 2007: fig. 1A), and *L. richterae* (~11%) (Sachs et al.,
324 2017: fig. 4); the Upper Cretaceous elasmosaurids *Z. oceanis* (~12%~13%) (Lomax and
325 Wahl, 2013: fig Vincent et al., 2011: fig. 2), *L. morgani* (~11%) (Sachs and Kear, 2017: fig.
326 1A, C), *T. keyesi* (~10%~8%) (O’Gorman et al., 2017: fig. 2), *T. haningtoni* (~9%)
327 (Carpenter, 1999: fig. 12), *S. snowii* (~9%) (Sachs et al., 2018: fig. 1), and *F. suzukii* (~5%)
328 (Sato et al., 2006: fig. 4); and the aristonectine elasmosaurids (~3%) (Otero et al., 2012,
329 2014), which have long skulls with an increased number of teeth.

330 There are other features that distinguish *L. bernardoi* from other comparable elasmosaurids,
331 mainly from those of the early Cretaceous, which are worth discussing. The position of the

332 external naris in *L. bernardoi* (at the level of the second maxillary position) differs from
333 that in *Z. oceanis* (first maxillary position) (Lomax and Wahl, 2013: fig 5; Vincent et al.,
334 2011: fig. 2) and those in *S. snowii*, *N. bradti* or *L. morgani* (third or posterior to the third
335 maxillary position) (Sachs and Kear, 2017: fig. 1C; Sachs et al., 2018; Serratos et al., 2017:
336 fig. 3). The absence of the dorsomedial ridge in the premaxillae of *L. bernardoi*, which is a
337 characteristic that it shares with *L. richterae* and *F. Suzukii* (Sachs et al., 2017; Sato et al.,
338 2006), differs from the keeled premaxillae that are found in most elasmosaurids, including
339 *C. colombiensis* (Figs. 4A, B, D), *E. australis* and *N. bradti* (Benson and Druckenmiller,
340 2014: character 17; Kear, 2007; Serratos et al., 2017; Welles, 1943, 1962). The size and
341 form of the external nares of *L. bernardoi* differ from the small cordate external nares of *N.*
342 *bradti* (Serratos et al., 2017). In *L. bernardoi*, the palatine participates only in the
343 posteromedial tip of the internal naris, while in *L. richterae*, the palatine forms the
344 posterolateral margin of the internal naris (Sachs et al., 2017: figs. 3A, B). In *L. bernardoi*,
345 the pterygoids are not visible between the vomers, while in *L. richterae* and in *M.*
346 *seymourensis*, the vomer has a posterior medial V-shaped notch from which the pterygoids
347 can be seen (Chatterjee and Small, 1989; O’Keefe et al., 2017; Sachs et al., 2017). *M.*
348 *seymourensis* also has in the vomer a medial ventral ridge (O’Keefe et al., 2017) that is
349 absent in *L. bernardoi*.

350 The normal ventral surface of the dentaries along the mandibular symphysis of *L. bernardoi*
351 differs from that of *L. richterae*, which exhibits a platform (Sachs et al., 2017: fig. 7); those
352 of *E. australis*, *Z. oceanis*, *L. morgani* and *S. snowii*, which have a symphyseal keel (Kear,
353 2007; Sachs and Kear, 2017; Sachs et al., 2018: fig. 3B, Vincent et al., 2011); that of *F.*
354 *suzukii*, which has a symphyseal pit (Sato et al., 2006); and those of *T. keyesi* and *C.*

355 *colombiensis*, which have a narrow symphyseal sulcus (Welles, 1962; O'Gorman et al.,
356 2017: fig. 9L). The symphyseal ventral groove, which is slightly marked in *L. bernardoi*, is
357 deep in *C. colombiensis* (Figs. 4C, E). The non-participation of the angular and splenial in
358 the mandibular symphysis distinguishes *L. bernardoi* from *S. snowii*, in which the angular
359 participates (Sachs et al., 2018), and from *N. bradti*, in which the splenial participates
360 (Serratos et al., 2017).

361 In the new specimen and in *C. colombiensis*, the first premaxillary alveolus is smaller than
362 the second and third, but the difference in size is more significant in *C. colombiensis* (Figs.
363 3D-E, H). On the other hand, in *N. bradti*, *T. keyesi* and *T. haningtoni*, the first
364 premaxillary alveolus is not significantly smaller than the third (Serratos et al., 2017;
365 Welles, 1943; Wiffen and Moisley, 1986), which differs from the condition that is found in
366 *L. bernardoi*. The alveoli of *L. bernardoi* are relatively larger than those of *C.*
367 *colombiensis*. This is evident for both, in the anterior view (Figs. 3A, B, D, E, H), and in
368 comparing the position of the tenth mandibular alveolus (Figs. 3C, F, G). This alveolus is
369 located near the middle of the orbit in *L. bernardoi* (Figs. 3F, G) but anterior to the anterior
370 margin of the orbit in the UCMP 38349 specimen of *C. colombiensis* (Fig. 3C). The
371 circular cross section of the teeth of *L. bernardoi* is shared with *L. richterae*, *E. australis*
372 and *C. colombiensis* (Kear, 2005; Sachs et al., 2017, Welles 1962) and differs from the
373 labiolingually compressed teeth of most of the Late Cretaceous elasmosaurids (Sachs and
374 Kear, 2017; Sachs et al., 2017; Sachs et al., 2018; Serratos et al., 2017: character 139) and
375 the “D” shaped tooth cross section of *N. bradti* (Serratos et al., 2017). The smooth texture
376 of the crown of *L. bernardoi* is similar to that of *C. colombiensis*, but in *L. bernardoi*, the
377 enamel has very slight ridges and transverse wrinkles towards the base of the crown, while

378 in *C. colombiensis*, it has anterior and posterior edges that are finely striated longitudinally
379 (Welles, 1962). Transverse wrinkles, which are similar to those of *L. bernardoi*, were
380 described for *L. morgani* (Welles, 1949), while in most elasmosaurids, the crowns show
381 more regular longitudinal ridges (Chatterjee and Small, 1989; Sachs et al., 2017; Sato,
382 2003; Sato et al., 2006; Serratos et al., 2017; Vincent et al., 2011; Wiffen and Moïseley,
383 1986).

384

385 **5.2 Phylogenetic analysis**

386 The Wagner tree search resulted in a subset of 5000 parsimonious trees (MPTs), and the
387 final phylogenetic analysis resulted in 20000 MPTs with 1502 steps (CI=0.273 and RI=
388 0.667). The strict consensus (Fig. 5A) recovers *L. bernardoi* within the Elasmosauridae
389 clade, which is identified only by postcranial synapomorphies. *L. bernardoi* is the sister
390 taxa of *T. keyesi* and *T. haningtoni*. This node (*L. bernardoi* + (*T. keyesi* + *T. haningtoni*))
391 is closely related to the node *L. morgani*+ (*S. snowii* + *H. alexandrae*), which forms a well-
392 resolved branch. In contrast, the basal elasmosaurids, including the Early Cretaceous *C.*
393 *colombiensis* and *E. australis*, as well as some Late Cretaceous elasmosaurids, were
394 recovered within polytomies that are only resolved after pruning unstable OTUs, which
395 were identified by applying the IterPCR algorithm (Figs. 5A-B). The elasmosaurids that
396 were identified as unstable OTUs were *E. australis*, *C. colombiensis*, *E. platyurus* and *Z.*
397 *oceanis*.

398 *L. bernardoi* is differentiated from the *T. keyesi* + *T. haningtoni* node by the absence of a
399 dorsomedian ridge in the premaxilla (17.0), which is a characteristic that is found in

400 leptocleidid plesiosauroids, and by the smaller size of the first premaxillary alveolus
401 (140.1), a characteristic also found in the closely related *L. morgani* + (*S. snowii* + *H.*
402 *alexandrae*) node. *L. bernardoii* is grouped with *T. keyesi* + *T. haningtoni* and is separated
403 from the *L. morgani* + (*S. snowii* + *H. alexandrae*) node by the reduced size of the
404 distalmost alveolus of the premaxilla (132.1). Altogether, these taxa form a branch that can
405 be distinguished from all of the other elasmosaurids by the posteromedian process of the
406 premaxilla not expanding into the original width posterior to the naris (22.1), and by two
407 postcranial synapomorphies that are unknown in *L. bernardoii*: there are more than 60
408 cervical vertebrae and pubis without anterolateral cornu.

409

410 **5.3 Dentition differences and trophic changes**

411 Elasmosaurids have largely been considered to be ecologically optimized to middle trophic-
412 level aquatic predation based on the presence of narrow tooth crowns with a markedly
413 elongated profile that indicates structural fragility (Massare, 1987; Kear et al., 2017).
414 However, even among elasmosaurids there is a clear tooth morphological variation.
415 Differences in related features, such as symphyseal length, number of symphyseal alveoli,
416 tooth shape and increase in the number of alveolar count, have been observed in the Late
417 Cretaceous aristonectines (*A. parvidens*, *Kaiwhekea katiki* Cruickshank and Fordyce, 2002)
418 and have been associated with differences in prey capture strategy and prey preference
419 compared with non-aristonectines (Cruickshank and Fordyce, 2002; O'Gorman, 2016;
420 Otero et al., 2014). Following the same argumentation line, the differences in dentition and
421 alveoli size between *L. bernardoii* and *C. colombiensis* (the alveoli of *L. bernardoii* are

422 larger than those of *C. colombiensis*; the mandible of *L. bernardoï* shows less alveoli than
423 those observed in *C. colombiensis*, and the symphysis of *L. bernardoï* is longer and bears
424 fewer teeth) appear to indicate a subdivision in prey preference between species from the
425 similar locality and age (late Aptian). These differences suggest specialization in the
426 feeding of the Early Cretaceous Colombian elasmosaurids, with *L. bernardoï* likely being
427 able to consume prey that are larger than those preferred by *C. colombiensis*.

428 It is interesting to remark that the decrease in tooth count was achieved several times during
429 the elasmosaurid history, as is recorded in *Z. oceanis* from the Maastrichtian of Morocco
430 (Lomax and Wahl, 2013; Vincent et al., 2011). Nevertheless, in *Z. oceanis*, the reduction in
431 tooth number is associated with a decrease in alveolar size (Lomax and Wahl, 2013, fig. 7,
432 8), which is not the case in *L. bernardoï*. Therefore, differences in the teeth number and
433 proportions that are observed in Cretaceous elasmosaurids seem to indicate changes in their
434 food preferences throughout their history. The contemporaneity of *L. bernardoï* and *C.*
435 *colombiensis* suggests that the elasmosaurids have achieved diverse prey preferences since
436 the Early Cretaceous, at least in the Colombian sea.

437

438 6. CONCLUSIONS

439 The new specimen FCG-CBP-22 is defined as a new genus and species of Elasmosauridae,
440 *Leivanectes bernardoï* gen. et sp. nov., by having large premaxillary alveoli and a
441 distinctive amount of alveoli in the different regions of the cranium and mandible. *L.*
442 *bernardoï* differs from other Lower Cretaceous elasmosaurids in that it has five
443 premaxillary alveoli, three pairs of alveoli on the mandibular symphysis, seven mandibular

444 alveoli anterior to the orbit, the tenth mandibular alveolus located near the level of the
445 middle of the orbit, the absence of a symphyseal ventral elaboration, and vomers that do not
446 form a posterior medial V-shaped notch to accommodate the pterygoids. *L. bernardoï*
447 represents the second elasmosaurid species that was defined from the Aptian of Colombia
448 and the Lower Cretaceous of South America.

449 The large alveoli of *L. bernardoï* allows for a feeding habit that relies on prey of greater
450 size than those chosen by others elasmosaurids, including *C. colombiensis*. Since both *L.*
451 *bernardoï* and *C. colombiensis* come from the upper Aptian beds of the same geographic
452 region, these differences suggest that the elasmosaurids could have attained a wide range of
453 morphologies during the Early Cretaceous, at least in the Colombian sea.

454

455 7. ACKNOWLEDGMENTS

456 We are grateful to the Centro de Investigaciones Paleontológicas (CIP) for allowing the
457 study of the fossil. We would like to thank Dr. Fernando Etayo-Serna for his comments on
458 the age of the fossil, and M. Pardo from the Museo Geológico José Royo y Gómez of the
459 Servicio Geológico Colombiano (SGC) for giving access to the material of *C.*
460 *Colombiensis*. Patricia Holroyd (UCPM) allowed for the revision of Colombian
461 elasmosaurid material under her care, for which we are grateful. The Doris and Samuel P.
462 Welles Grant supported the visit of JPO'G to the UCPM. The author also thanks Jorge
463 Gonzalez for some of the illustrations. This work was partially supported by the PICT
464 2015-0678 to J.P.O'G. TNT is a free program that is available with the sponsorship of the

465 Willi Hennig Society. We sincerely thank Patrick Druckenmiller and Benjamin P. Kear for
466 their useful comments on the manuscript, which enhanced this version.

467 8. REFERENCES

468 Benson, R. B. J., Druckenmiller, P. S., 2014. Faunal turnover of marine tetrapods during the
469 Jurassic-Cretaceous transition. *Biological Reviews of the Cambridge Philosophical*
470 *Society* 89, 1-23.

471 Blainville, H. D. de., 1835. Description de quelques espèces de reptiles de la Californie,
472 précédée de l'analyse d'un système général d'herpetologie et d' amphibiologie.
473 *Nouvelles Archives Du Museum d'Histoire Naturelle* 4, 233-296.

474 Bremer, K., 1994. Branch support and tree stability. *Cladistics* 10, 295-304.

475 Brown, D. S., 1981. The English Upper Jurassic Plesiosauroidea (Reptilia) and a review of
476 the phylogeny and classification of the Plesiosauria. *Bulletin of the British Museum of*
477 *Natural History (Geology)* 35(4), 253-347.

478 Cabrera, A., 1941. Un plesiosaurio nuevo del Cretáceo del Chubut. *Revista del Museo de*
479 *La Plata* 2, 113-130.

480 Carpenter, K., 1997. Comparative cranial anatomy of two North American plesiosaurs. In:
481 Callaway, J.M., Nicholls, E.L. (Eds.), *Ancient Marine Reptiles*. Academic Press, San
482 Diego, 191-216.

483 Carpenter, K., 1999. Revision of North American elasmosaurs from the Cretaceous of the
484 Western Interior. *Paludicola* 2, 148-173.

485 Chatterjee, S., Small, B. J., 1989. New plesiosaurs from the Upper Cretaceous of
486 Antarctica. *Special Publication of the Geological Society of London* 47, 197-215

- 487 Cope, E. D., 1868. Remarks on a new enaliosaurian, *Elasmosaurus platyurus*. Proceedings
488 of the Academy of Natural Sciences of Philadelphia 1868, 92-93.
- 489 Cope, E. D., 1869. Extinct Batrachia, Reptilia and Aves of North America. Transactions of
490 the American Philosophical Society 14, 1-252.
- 491 Cruickshank, A. R., Fordyce, R. E., 2002. A new marine reptile (Sauropterygia) from New
492 Zealand: further evidence for a Late Cretaceous austral radiation of cryptoclidid
493 plesiosaurs. *Palaeontology* 45, 557-575.
- 494 Etayo-Serna, F., 1968. El sistema Cretáceo en la región de Villa de Leiva y zonas próximas.
495 *Geología Colombiana* 5, 5-74.
- 496 Etayo-Serna, F., 1979. Zonation of the Cretaceous of Central Colombia by ammonites.
497 *Publicaciones Geológicas Especiales del INGEOMINAS* 2, 1-186.
- 498 Farris, J. S., 1989. The retention index and the rescaled consistency index. *Cladistics* 5,
499 417- 419.
- 500 Forero, H. and Sarmiento, L. F., 1985. La facies evaporítica de la Formación Paja en la
501 región de Villa de Leiva. In: Etayo-Serna, F., Laverde, F. (Eds), Proyecto Cretácico-
502 Contribuciones. *Publicaciones Geológicas Especiales del INGEOMINAS*, Bogotá,
503 Colombia, XVII1-XVII16.
- 504 Gómez-Pérez, M. and Noè, L. F., 2017. Cranial anatomy of a new pliosaurid *Acostasaurus*
505 *pavachoquensis* from the Lower Cretaceous of Colombia, South America,
506 *Palaeontographica Abteilung A.* 310, 5-42.
- 507 Goñi, R., Gasparini, Z., 1983. Nuevos restos de '*Alzadasaurus colombiensis*' (Reptilia,
508 Plesiosauria) del Cretácico temprano de Colombia. *Geología Norandina* 7, 49-54.

- 509 Goloboff, P. A., Catalano, S. A., 2016. TNT version 1.5, including a full implementation of
510 phylogenetic morphometrics. *Cladistics* 32, 221-238.
- 511 Kear, B. P., 2005. A new elasmosaurid plesiosaur from the Lower Cretaceous of
512 Queensland, Australia. *Journal of Vertebrate Paleontology* 25, 792-805.
- 513 Kear, B. P., 2007. Taxonomic clarification of the Australian elasmosaurid genus
514 *Eromangasaurus*, with reference to other austral elasmosaur taxa. *Journal of Vertebrate*
515 *Paleontology* 27(1), 241-246.
- 516 Kear, B. P., Larsson, D., Lindgren, J., Kunderát, M., 2017. Exceptionally prolonged tooth
517 formation in elasmosaurid plesiosaurians. *PloS one*, 12, e0172759.
- 518 Ketchum, H. F., Benson, R. B. J., 2010. Global interrelationships of Plesiosauria (Reptilia,
519 Sauropterygia) and the pivotal role of taxon sampling in determining the outcome of
520 phylogenetic analyses. *Biological Reviews* 85, 361-392.
- 521 Lomax, D. R., Wahl, W., 2013. A new specimen of the elasmosaurid plesiosaur
522 *Zarafasaura oceanis* from the Upper Cretaceous (Maastrichtian) of Morocco. *Paludicola*
523 9(2), 97-109.
- 524 Maddison, W. P., Maddison, D. R., 2011. Mesquite: a modular system for evolutionary
525 analysis. Version 2.75.
- 526 Massare, J. A., 1987. Tooth morphology and prey preference of Mesozoic marine reptiles.
527 *Journal of Vertebrate Paleontology* 7(2), 121-137.
- 528 Maxwell, E. E., Dick, D., Padilla, S., Parra, M.L., 2015. A new ophthalmosaurid
529 ichthyosaur from the Early Cretaceous of Colombia. *Papers in Palaeontology*.
530 doi.org/10.1002/spp2.1030.
- 531 O’Gorman, J. P., 2016. New Insights on the *Aristonectes parvidens* (Plesiosauria,

- 532 Elasmosauridae) Holotype: News on an Old Specimen. *Ameghiniana* 53, 397-417.
- 533 O’Gorman, J. P., Otero, R. A., Hiller, N., Simes, J., Terezow, M., 2017. Redescription of
534 *Tuarangisaurus keyesi* (Sauropterygia; Elasmosauridae), a key species from the
535 uppermost Cretaceous of the Weddellian Province: internal skull anatomy and
536 phylogenetic position. *Cretaceous Research* 71, 118-136.
- 537 O’Keefe, F. R., 2001. A cladistic analysis and taxonomic revision of the Plesiosauria
538 (Reptilia: Sauropterygia). *Acta Zoologica Fennica* 213, 1-63.
- 539 O’Keefe, F. R., Otero, R. A., Soto-Acuña, S., O’Gorman, J. P., Godfrey, S. J., Chatterjee,
540 S., 2017. Cranial anatomy of *Morturneria seymourensis* from Antarctica, and the
541 evolution of filter feeding in plesiosaurs of the Austral Late Cretaceous. *Journal of*
542 *Vertebrate Paleontology* 37.4, e1347570, DOI: 10.1080/02724634.2017.1347570.
- 543 Otero, R. A., 2016. Taxonomic reassessment of *Hydralmosaurus* as *Styxosaurus*: new
544 insights on the elasmosaurid neck evolution throughout the Cretaceous. *PeerJ* 4, 1-60
- 545 Otero, R. A., Soto-Acuña, S., Rubilar-Rogers, D., 2012. A postcranial skeleton of an
546 elasmosaurid plesiosaur from the Maastrichtian of central Chile, with comments on the
547 affinities of Late Cretaceous plesiosauroids from the Weddellian Biogeographic
548 Province. *Cretaceous Research* 37, 89-99.
- 549 Otero, R. A., Soto-Acuña, S., O’Keefe, F. R., O’Gorman, J. P., Stinnesbeck, W. S., Suárez,
550 M. E., Rubilar-Rogers, D., Salazar, C., Quinzio-Sinn, L. A., 2014. *Aristonectes*
551 *quiriquinensis*, sp. nov., a new highly derived elasmosaurid from the upper
552 Maastrichtian of central Chile. *Journal of Vertebrate Paleontology* 34, 100-125.
- 553 Owen, R., 1860. On the orders of fossil and recent Reptilia, and their distribution in time.

- 554 Reports of the British Association for the Advancement of Science 29, 153-166.
- 555 Padilla, C. B., Páramo, M. E., Noè, L., Gómez Pérez, M., Parra, M. L., 2010). Acid
556 preparation of large vertebrate specimens. The Geological Curator 9 (3), 213-220.
- 557 Páramo-Fonseca, M. E., 2015. Estado actual del conocimiento de los reptiles marinos
558 cretácico de Colombia. En: Fernández, M. y Herrera, Y. (Eds.) Reptiles Extintos -
559 Volumen en Homenaje a Zulma Gasparini. Publicación Electrónica de la Asociación
560 Paleontológica Argentina 15, 40-57. <http://dx.doi.org/10.5710/PEAPA.12.06.2015.98>.
- 561 Páramo-Fonseca, M. E., Gómez-Pérez, M., Noé, L. F., Etayo-serna, F., 2016.
562 *Stenorhynchosaurus munozi*, gen. et sp. nov. a new pliosaurid from the upper Barremian
563 (Lower Cretaceous) of Villa de Leiva, Colombia, South America, Revista de la
564 Academia Colombiana de Ciencias Exactas, Físicas y Naturales 40, 84-103.
- 565 Pol, D., Escapa, I. H., 2009. Unstable taxa in cladistic analysis: identification and the
566 assessment of relevant characters. Cladistics 25, 515-527.
- 567 Sachs, S., 2005a. *Tuarangisaurus australis* sp. nov. (Plesiosauria: Elasmosauridae) from
568 the Lower Cretaceous of northeastern Queensland, with additional notes on the
569 phylogeny of the Elasmosauridae. Memoirs of the Queensland Museum 50, 425-440.
- 570 Sachs, S., 2005b. Redescription of *Elasmosaurus platyurus* Cope 1868 (Plesiosauria:
571 Elasmosauridae) from the Upper Cretaceous (lower Campanian) of Kansas, U.S.A.
572 Paludicola 5, 92-106.
- 573 Sachs, S., Hornung, J. J., Kear, B. P., 2017. A new basal elasmosaurid (Sauropterygia:
574 Plesiosauria) from the Lower Cretaceous of Germany. Journal of Vertebrate
575 Paleontology 37, e1301945.

- 576 Sachs, S., Lindgren, J., Kear, B. P., 2018. Reassessment of the *Styxosaurus snowii*
577 (Williston, 1890) holotype specimen and its implications for elasmosaurid plesiosaurian
578 interrelationships. *Alcheringa*. 1-27. *In press*, DOI: 10.1080/03115518.2018.1508613
- 579 Sato, T., 2003. *Terminonatator ponteixensis*, a new elasmosaur (Reptilia; Sauropterygia)
580 from the Upper Cretaceous of Saskatchewan. *Journal of Vertebrate Paleontology* 23, 89-
581 103.
- 582 Sato, T., Hasegawa, Y., Manabe, M., 2006. A new elasmosaurid plesiosaur from the Upper
583 Cretaceous of Fukushima, Japan. *Palaeontology* 49, 467-484.
- 584 Serratos, D. J., Druckenmiller, P., Benson, R. B., 2017. A new elasmosaurid
585 (Sauropterygia, Plesiosauria) from the Bearpaw Shale (Late Cretaceous, Maastrichtian)
586 of Montana demonstrates multiple evolutionary reductions of neck length within
587 Elasmosauridae. *Journal of Vertebrate Paleontology*, e1278608.
- 588 Smith, J., Dodson, P., 2003. A proposal for a standard terminology of anatomical notation
589 and orientation in fossil vertebrate dentitions. *Journal of Vertebrate Paleontology* 23 (1),
590 1-12.
- 591 Vincent, P., Bardet, N., Pereda-Suberbiola, X., Bouya, B., Amaghaz, M., Meslouh, S.,
592 2011. *Zarafasaura oceanis*, a new elasmosaurid (Reptilia: Sauropterygia) from the
593 Maastrichtian Phosphates of Morocco and the palaeobiogeography of latest Cretaceous
594 plesiosaurs. *Gondwana Research* 19, 1062-1073.
- 595 Welles, S. P., 1943. Elasmosaurid plesiosaurs with description of new material from
596 California and Colorado. *Memoirs of the University of California* 13, 125-254.
- 597 Welles, S. P., 1949. A new elasmosaur from the Eagle Ford Shale of Texas. *Fondren*

598 Science Series 1, 1-28.

599 Welles, S. P., 1952. A review of the North American Cretaceous elasmosaurs. University of
600 California Publications in Geological Sciences 29, 47-143.

601 Welles, S. P., 1962. A new species of elasmosaur from the Aptian of Colombia and a
602 review of the Cretaceous plesiosaurs. University of California, Publications in
603 Geological Sciences 44, 1-96. Wiffen, J., Moislley, W. L., 1986. Late Cretaceous reptiles
604 (Families Elasmosauridae and Pliosauridae) from the Mangahouanga Stream, North
605 Island, New Zealand. New Zealand Journal of Geology and Geophysics 29, 205-252.

606 Williston, S. W., 1890. A new plesiosaur from the Niobrara Cretaceous of Kansas.
607 Transactions of the Kansas Academy of Science 13, 107-111.

608

609 **APPENDIX I**

610 Character states of *Leivanectes bernardoii* gen. et sp. nov.

611 00?????1? 0?00?0?0 0100?000? ??00????? ???? ?????? ?????????? ??????????

612 ?????????? ?????????? 10000????? ?????????? ?100????? 0??01?0?? 1110011001

613 ?????????? ?????????? ?????????? ?????????? ?????????? ?????????? ??????????

614 ?????????? ?????????? ?????????? ?????????? ?????????? ??????????

615

616

617 Figure captions

618 Figure 1. Geographic and stratigraphic provenance of the holotype specimen FCG-CBP-22
619 of *Leivanectes bernardoii* gen. et sp. nov. A, locality where FCG-CBP-22 was collected
620 (arrow). B, generalized stratigraphic column of the Paja Formation showing the specimen

621 occurrence (modified from Etayo-Serna, 1979). C, lateral and ventral views of
622 *Chelonicerias (Epicheloniceras) carlosacostai* Etayo-Serna, 1979 (FCG-CBP-46) found
623 with the skeletal remains (scale bar = 5mm).

624

625 Figure 2. *Leivanectes bernardoi* gen. et sp. nov., holotype (FCG-CBP-22), A-D,
626 photographs and interpretative drawings of skull and mandible in anterior (A), left lateral
627 (B), dorsal (C) and ventral (D) views. Dashed lines: interpretative limits (Scale bar = 20
628 mm). E, photograph of the fourth right premaxillary tooth in lateral view (Scale in cm).

629 Abbreviations: **1st**, **2nd**, ..., premaxillary alveolus; **a**, angular; **c**, coronoid; **de**, dentary; **fr**,
630 frontal; **mx**, maxilla; **p**, parietal; **pl**, palatine; **pmx**, premaxilla; **pof**, postfrontal; **prf**,
631 prefrontal; **pt**, pterygoid; **sp**, splenial; **v**, vomer.

632

633

634 Figure 3. A-B, plot of mesio-distal length of premaxillary alveoli of *L. bernardoi* (FCG-
635 CBP-22), *C. colombiensis* (UCMP 125328) and *T. keyesi* (NPC CD 425),
636 100*AMD/preorbital length (A), and, absolute measures (AMD) (B). C-H, comparison of
637 alveolar features between the *C. colombiensis* holotype (UCMP 38349), referred specimen
638 (UCMP 125328) and holotype of *L.bernardoi* FCG-CBP-22. C and F, the anterior orbital
639 margin (vertical line) and the tenth mandibular alveoli (arrow) in *C. colombiensis* holotype
640 (C) and *L. bernardoi* (F, G). D, E and H, comparison of anterior views of *C. colombiensis*,
641 holotype (D) and referred specimen (E), and *L. bernardoi* (H) (Scale bars = 20mm).

642

643 Figure 4. *C. colombiensis* skull and mandible. A-D, holotype (UCMP 38349) in right lateral
644 (A), left lateral (B), ventral (C) and dorsal (D) views. E-F, referred specimen (UCMP
645 125328) in ventral (E) and dorsal (F) views (Scale bars = 20 mm). Abbreviations: **pmr**,
646 premaxillary ridge; **svg**, symphyseal ventral groove.

647

648

649 Figure 5. A-B, Plesiosauroidea branch from the phylogenetic analysis of Plesiosauria data
650 set (See material and Methods). A, strict consensus of 20000 most parsimonious trees, 1502
651 steps, obtained after (TBR) branch swapping. Bremer Support indicated below some nodes.
652 B, reduced most parsimonious tree after pruning unstable taxa (Plesiosauroidea pruned
653 OTUs: *Hastanectes valdensis*, *Callawayasaurus colombiensis*, *Eromangasaurus australis*,
654 *Elasmosaurus platyurus* and *Zarafasaura oceanis*).

655

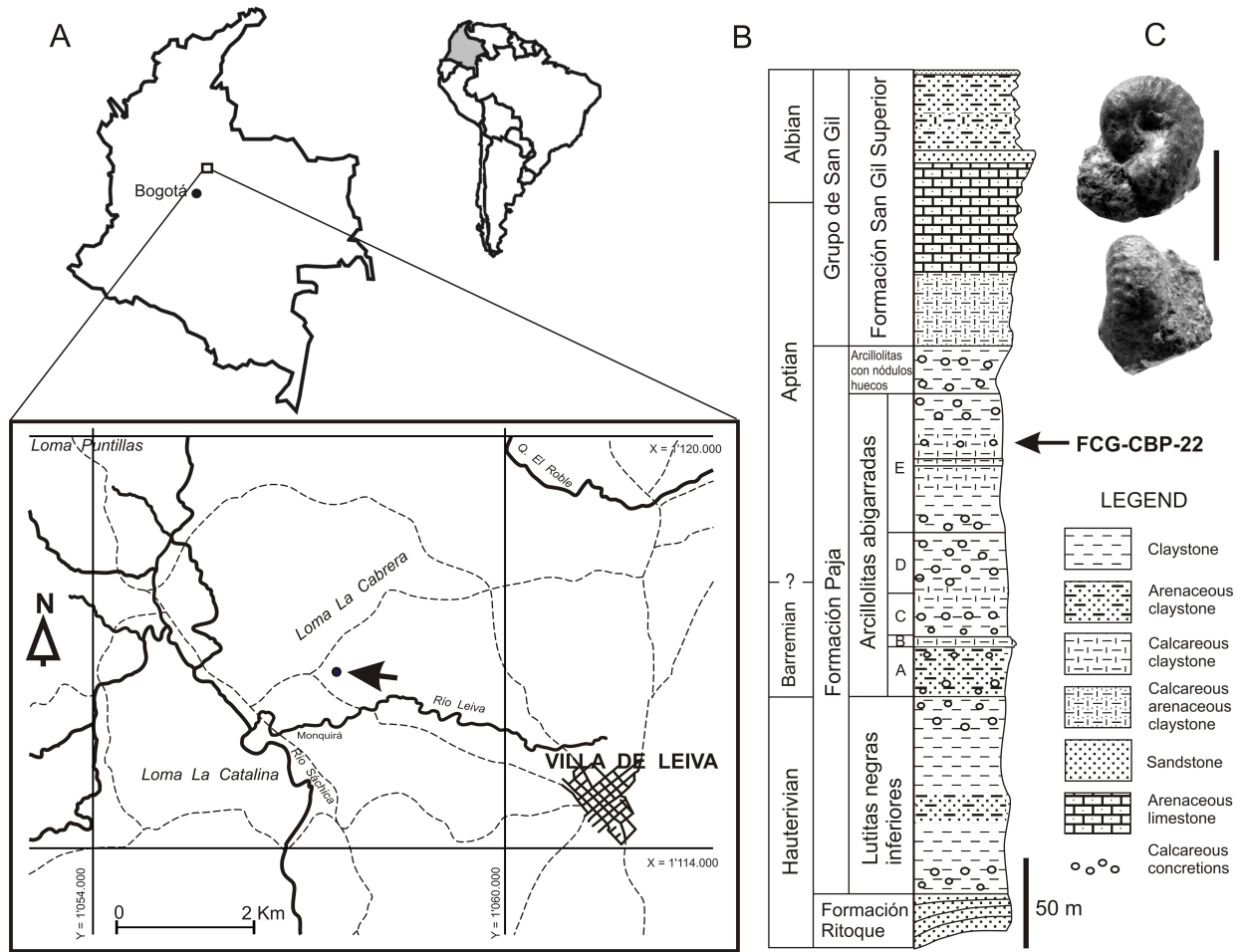
656 Table 1. Mesodistal measurements of the premaxillary and maxillary alveoli (in mm). The
657 maxillary alveoli measurements were taken from the left side of the skull.

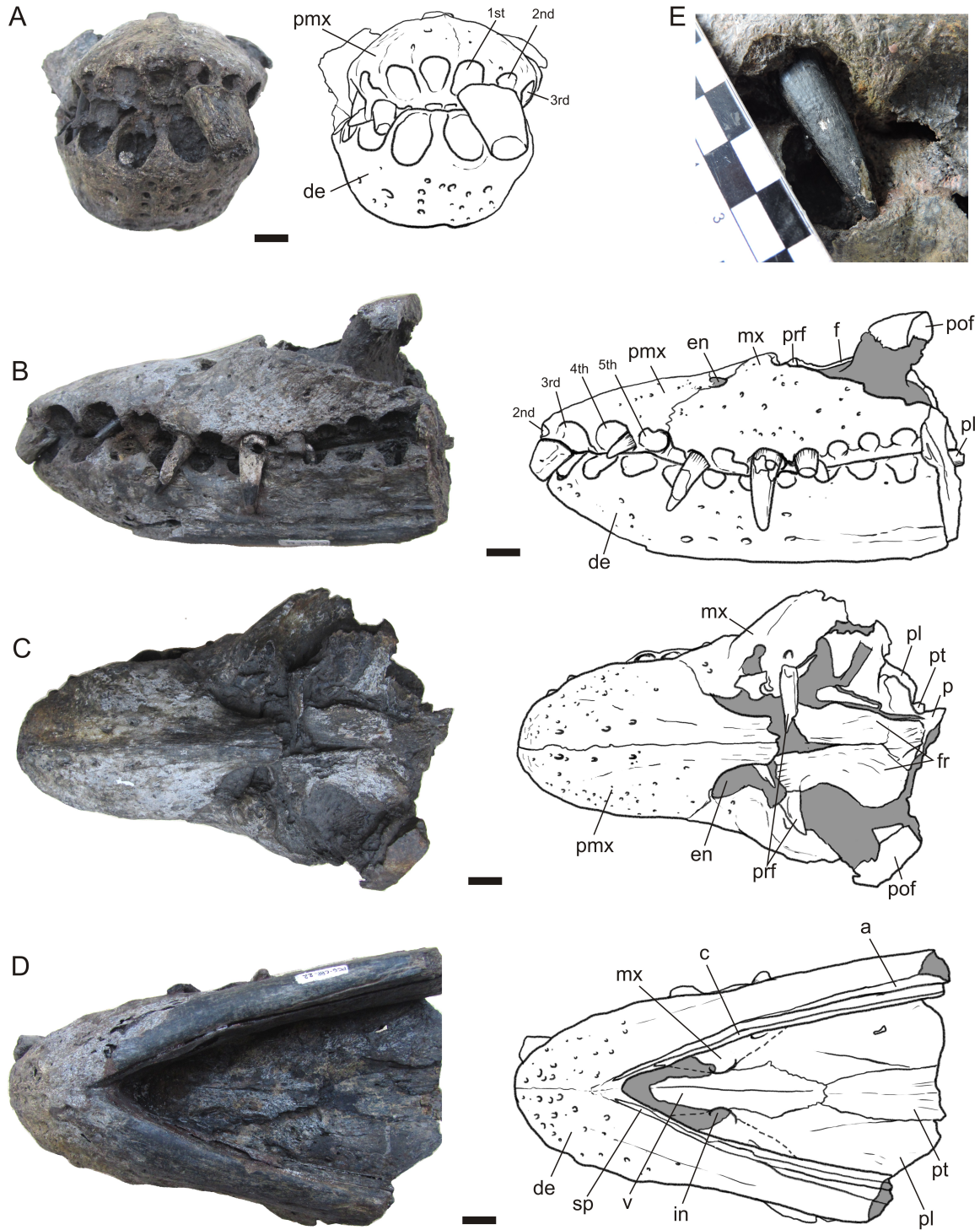
658

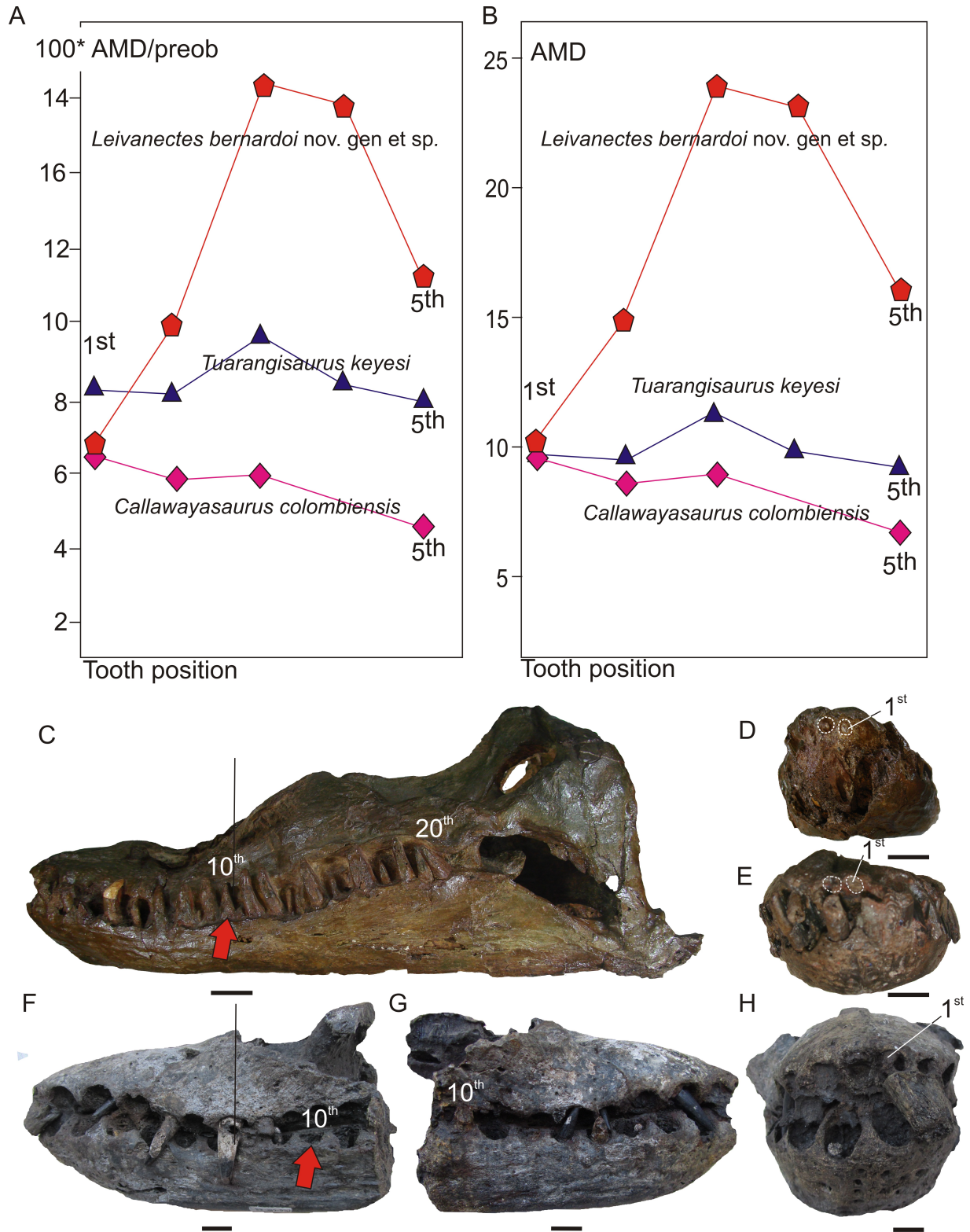
659 Table 2. Alveolar account of several elasmosaurids (data Taken from Carpenter, 1997: fig.
660 2; Kear, 2005, 2007; Lomax and Wahl, 2013; O'Gorman et al., 2017: fig. 7A, B, 9M; Otero,
661 2016; Sachs et al., 2017; Sachs et al., 2018: fig. 1B; Sato, 2003: fig. 5; Sato et al., 2006: fig.
662 4A; Serratos et al., 2017: fig. 3, 4; Vincent et al., 2011: fig. 4A;; Welles, 1943, 1949, 1962;
663 J.P.O'G pers. obs.).

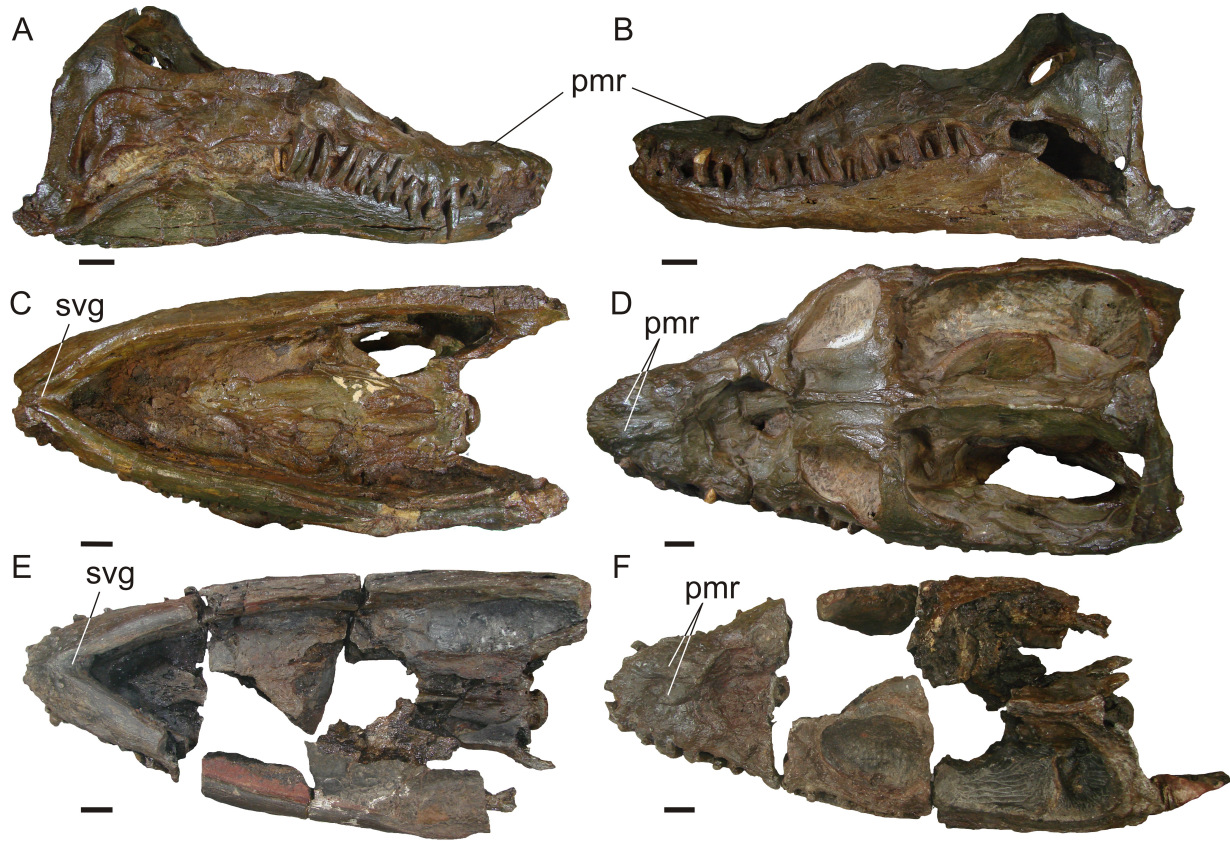
Premaxillary alveolus	Mesodistal measurement	Maxillary alveolus	Mesodistal measurement	Maxillary alveolus	Mesodistal measurement
1 st	10	1 st	9	6 th	18
2 nd	15	2 nd	14	7 th	13
3 rd	24	3 rd	20	8 th	11
4 th	23	4 th	21	9 th	13
5 th	16	5 th	21		

Elasmosaurid species	Number of symphyseal alveoli	Number of premaxillari alveoli	Number of pre-orbital alveoli in mandible
<i>Leivanectes bernardoii</i> gen. at sp. nov. (FCG-CBP-22)	3	5	7
<i>Eromangasaurus australis</i> (QM F11050)	~5	4 (left)/ 3(right)	7+
<i>Callawayasaurus colombiensis</i> (UCMP 38349, holotype; UCMP 125328 referred)	~5-6	5	~11
<i>Libonectes morgani</i> (SMUSMP 69120)	4	5	10
<i>Thalassomedon hanningtoni</i> (UNSM 50132)	?	5?	~10
<i>Futabasaurus suzukii</i> (NSM PV15025)	~4	5	~12
<i>Zarafasaura oceanis</i> (OCP DEK/GE 315)	~4	4-5	7?
<i>Tuarangisaurus keyesi</i> (NPC CD 425)	4	5	10
<i>Terminonatator ponteixensis</i> (RSM P2414.1)	3	4 left/1midline/4 right	~10
<i>Lagenanectes richterae</i> (BGR Ma 13328)	4	5	8+, ~13
<i>Styxosaurus browni</i> (AMNH 5835)	?	4-5	9+
<i>Styxosaurus snowii</i> (KUVV 1301)	3	5	8+
<i>Nakanectes bradti</i>	3	5	~8









ACCEPTED MANUSCRIPT

